The Journal of Immunology

Dendritic Cells of Mesenteric and Regional Lymph Nodes Contribute to *Yersinia enterocolitica* O:3–Induced Reactive Arthritis in *TNFRp55*$^{-/-}$ Mice

Juan E. Silva, Andrea C. Mayordomo, Mabel N. Dave, Claudia Aguilera Merlo, Ricardo J. Eliçabe and María S. Di Genaro

J Immunol published online 2 March 2020
http://www.jimmunol.org/content/early/2020/02/28/jimmunol.1901137

The Journal of Immunology is published twice each month by The American Association of Immunologists, Inc., 1451 Rockville Pike, Suite 650, Rockville, MD 20852

Print ISSN: 0022-1767 Online ISSN: 1550-6606.

Published March 2, 2020, doi:10.4049/jimmunol.1901137

Dendritic Cells of Mesenteric and Regional Lymph Nodes Contribute to *Yersinia enterocolitica* O:3–Induced Reactive Arthritis in *TNFRp55*$^{-/-}$ Mice

Juan E. Silva,*,† Andrea C. Mayordomo,† Mabel N. Dave,† Claudia Aguilera Merlo,* Ricardo J. Eliçabe,*,† and María S. Di Genaro*,†

Dendritic cells (DCs) participate in the pathogenesis of several diseases. We investigated DCs and the connection between mucosa and joints in a murine model of *Yersinia enterocolitica* O:3–induced reactive arthritis (ReA) in *TNFRp55*$^{-/-}$ mice. DCs of mesenteric lymph nodes (MLN) and joint regional lymph nodes (RLN) were analyzed in *TNFRp55*$^{-/-}$ and wild-type mice. On day 14 after *Y. enterocolitica* infection (arthritis onset), we found that under TNFRp55 deficiency, migratory (MHC^{high}CD11c^{+}) DCs increased significantly in RLN. Within these RLN, resident (MHC^{int}CD11c^{+}) DCs increased on days 14 and 21. Similar changes in both migratory and resident DCs were also detected on day 14 in MLN of *TNFRp55*$^{-/-}$ mice. In vitro, LPS-stimulated migratory *TNFRp55*$^{-/-}$ DCs of MLN increased IL-12/23p40 compared with wild-type mice. In addition, *TNFRp55*$^{-/-}$ bone marrow–derived DCs in a *TNFRp55*$^{-/-}$ MLN microenvironment exhibited higher expression of CCR7 after *Y. enterocolitica* infection. The major intestinal DC subsets (CD103^{+}CD11b^{-}, CD103^{-}CD11b^{+}, and CD103^{+}CD11b^{+}) were found in the RLN of *Y. enterocolitica*–infected *TNFRp55*$^{-/-}$ mice. Fingolimod (FTY720) treatment of *Y. enterocolitica*–infected mice reduced the CD11b^{-} subset of migratory DCs in RLN of *TNFRp55*$^{-/-}$ mice and significantly suppressed the severity of ReA in these mice. This result was associated with decreased articular IL-12/23p40 and IFN-γ levels. In vitro FTY720 treatment downregulated CCR7 on *Y. enterocolitica*–infected bone marrow–derived DCs and purified MLN DCs, which may explain the mechanism underlying the impairment of DCs in RLN induced by FTY720. Taken together, data indicate the migration of intestinal DCs to RLN and the contribution of these cells in the immunopathogenesis of ReA, which may provide evidence for controlling this disease. *The Journal of Immunology*, 2020, 204: 000–000.

Reactive arthritis (ReA) is a form of peripheral spondyloarthritis (SpA) that develops after a gastrointestinal or urogenital infection (1). The incidence range of ReA has been reported between 1 and 30 cases/100,000 per year, the frequency of which depends on the geographic area. ReA manifests ∼1–3 wk after the mucosal infection (2). Once ReA is detected, bacterial cultures of fluids are often negative, and usually, the Ag cannot be found in the joints (2). Although the coexistence of gut and joint inflammation is well established in SpA (3), the immunopathogenic mechanisms of this connection in ReA are currently unknown.

Yersinia enterocolitica are Gram-negative bacteria that cause food-born gastrointestinal diseases, including diarrhea, mesenteric lymphadenitis, and terminal ileitis. Moreover, *Y. enterocolitica* is a well-established trigger of ReA (4). Following the ingestion of contaminated food or water, *Y. enterocolitica* first colonize the lumen and transmigrate through Ag-sampling M cells across follicle-associated epithelium of the small intestine. This results in the colonization of Peyer's patches (PP) (5). Subsequently, *Y. enterocolitica* can spread via the lymph and/or blood into the mesenteric lymph nodes (MLN), where the bacteria cause inflammatory changes and from where *Y. enterocolitica* can invade internal organs, such as the liver and the spleen (5). Alternatively, the bacteria may use a PP-independent dissemination route and spread directly from the intestine to systemic tissues (6). *Y. enterocolitica* serotype O:3 is less virulent in mice than other serotypes, such as the serotype O:8. However, it is frequently isolated from patients and also associated with ReA (7).

TNF is a pleiotropic cytokine and a master regulator of the immune system, which plays important roles in homeostasis and inflammation (8). TNF mediates its function through two receptors: TNFRp55 (TNFRp55, TNFR1, or CD120a) and TNFRp75 (TNFR2 or CD120b). TNFRp55 is constitutively and ubiquitously expressed on a broad variety of cells, whereas expression of

*Facultad de Química, Bioquímica y Farmacia, Universidad Nacional de San Luis, 5700 San Luis, Argentina; and †Instituto Multidisciplinario de Investigaciones Biológicas-San Luis, Consejo Nacional de Investigaciones Científicas y Técnicas-Universidad Nacional de San Luis, 5700 San Luis, Argentina

ORCIDs: 0000-0002-0399-9644 (A.C.M.); 0000-0001-9854-5786 (M.S.D.G.).

Received for publication September 18, 2019. Accepted for publication January 24, 2020.

This work was supported by grants from the National Agency for Promotion of Science and Technology (PICT-2011-0732 and PICT-2017-2828), the National University of San Luis (PROICO-02-1218), the Alexander von Humboldt Foundation, and the National Council of Scientific and Technical Investigations (CONICET)–Deutsche Forschungsgemeinschaft cooperation project. R.J.E. and M.S.D.G. are members of the Scientific Career of CONICET; J.E.S., A.C.M., and M.N.D. are CONICET fellows.

J.E.S. and M.S.D.G. conceived the work. J.E.S. and M.S.D.G. designed the experiments. J.E.S., A.C.M., and M.N.D. performed the experiments. C.A.M. performed the histological studies. J.E.S., A.C.M., and R.J.E. analyzed the data. M.S.D.G. and J.E.S. wrote the manuscript and prepared the figures. All the authors revised and edited the manuscript.

Address correspondence and reprint requests to Dr. María S. Di Genaro, Laboratorio de Inmunopatología, Universidad Nacional de San Luis, Ejército de los Andes 950, 5700 San Luis, Argentina. E-mail address: sdigena@unsl.edu.ar

Abbreviations used in this article: BMDC, bone marrow–derived DC; DC, dendritic cell; FTY720, fingolimod; HEV, high endothelial venule; MLN, mesenteric lymph node; MLN me, MLN microenvironment; MLN me-day 14, MLN me on day 14; moi, multiplicity of infection; pi, postinfection; PP, Peyer's patch; pre-DC, precursor to DC; ReA, reactive arthritis; RLN, regional lymph node; SpA, spondyloarthritis; WT, wild-type; *Y. enterocolitica* O:3–GFP, GFP-expressing *Y. enterocolitica* O:3.

TNFR2 is inducible and tightly regulated (8). In previous studies, we have demonstrated that TNFRp55 is essential for the protection against both *Y. enterocolitica* infection and *Y. enterocolitica*–induced ReA through mechanisms that involve IL-12/23p40 production (9, 10).

Dendritic cells (DCs) are APCs that play powerful roles orchestrating innate and adaptive immune responses. They also maintain tissue tolerance or promote immune responses to pathogens (11). DCs are phagocytic cells that continuously sample Ags from their microenvironment. After the uptake of the Ag, DCs migrate to the draining lymph nodes, where they present this Ag to naive T lymphocytes. This migration is guided by the interaction of CCR7 on migrating DCs with its corresponding ligand CCL21, which is found on lymphatic endothelial cells (11).

A link between the intestine and joint inflammation is clear in ReA because this disease develops after a gastrointestinal infection (12). In previous research, bacterial products from a preceding gut infection were recovered from the joints of patients who developed ReA (12, 13). In addition, signaling through TNFRp55 has been previously shown to be essential for the development of both bowel inflammation and arthritis (14). However, the cellular targets of TNF remain poorly defined. DCs are also found throughout the intestine, including MLN, in which $CD103^+$ DCs, cells absent in the spleen, represent a population that migrates from the intestine lamina propria (15). Recently, we have reported that DCs are the main cellular source of high IL-12/23p40 levels in the pathophysiological scenario of *Y. enterocolitica*–induced ReA in TNFRp55-deficient ($TNFRp55^{-/-}$) mice (16). However, to the best of our knowledge, the role of DCs in the intestine–joint connection in ReA has not been previously explored. In this study, we investigated DCs of MLN and joint-draining lymph nodes (regional lymph nodes [RLN]) during the development of *Y. enterocolitica*–induced ReA in $TNFRp55^{-/-}$ mice. Moreover, we modulated DC trafficking to determine whether ReA can be suppressed by hindering the migration of DCs. Our data provide insights into the role of DCs in the joint–gut relationship in ReA. A deeper understanding of this connection could open new ways for controlling the development of ReA after an intestinal infection.

Materials and Methods

Mice

C57BL/6 $TNFRp55^{-/-}$ mice were kindly provided by the Max von Pettenkofer-Institute (Munich, Germany). C57BL/6 wild-type (WT) mice were purchased from the Animal Facilities of the National University of La Plata (La Plata, Argentina). Breeding colonies were established at the Animal Facilities of the National University of San Luis. Mice were kept under specific pathogen-free conditions in positive-pressure cabinets (EHRET, Emmendingen, Germany) and provided with sterile food and water ad libitum. Six- to eight-week-old male mice were used for the experiments. Experimental protocols were approved by the Animal Care and Use Committee of the National University of San Luis (San Luis, Argentina) (protocols number B-163/13).

Bacterial culture and in vivo infection

Strain MHC 700 *Y. enterocolitica* O:3 (kindly provided by Dr. G. Kapperud, Department of Bacteriology, National Institute of Public Health, Oslo, Norway) was used for infection. Bacteria were cultured as described by Di Genaro et al. (9). For tracking DC migration, GFP-expressing *Y. enterocolitica* O:3 (*Y. enterocolitica* O:3–GFP) was constructed by transforming this strain with the plasmid pACYC184 harboring the *gfp* gene (17). Transformation was carried out by electroporation as previously described (18). Mice were starved for 3 h and then infected orogastrically with $1–5 \times 10^8$ yersiniae in 200 μl of saline using a gastric tube. The control group received saline instead. The number of inoculated bacteria was controlled by plating serial dilutions of the inoculated suspension on Mueller–Hinton agar and counting of CFU following incubation at 27°C for 48 h.

In vitro infection

Bone marrow–derived DCs (BMDCs) were obtained according to Lutz et al. (19) protocols. Briefly, 2×10^6 bone marrow cells from femurs and tibias of C57BL6 WT or C57BL6 $TNFRp55^{-/-}$ mice were cultured in 100-mm dishes with supplemented RPMI 1640 medium: 10% FBS, 2 mM L-glutamine, 1 mM pyruvate, 100 IU/ml penicillin, and 100 μg/ml streptomycin. This contained 200 U of GM-CSF (Recombinant Murine GM-CSF; PeproTech, Rocky Hill, NJ). Three days after seeding, 10 ml of fresh medium with GM-CSF was added. Then, every 2 d, half of the medium is discarded and replaced by fresh medium. At days 8 and 9, the cells were analyzed by flow cytometry and more than 90% expressed CD11c marker. In addition, in vivo expansion and isolation of DCs from MLN (MLN DCs) were performed as previously described (16). For infection, 2×10^5 BMDCs or MLN DCs were seeded in 24-well plates in supplemented RPMI 1640 medium without antibiotics and infected with *Y. enterocolitica* O:3 in a multiplicity of infection (moi) of 10. After 1 h, 0.1 μg/ml of gentamicin was added to kill extracellular bacteria. Then, the BMDCs were cultured by 24 h for additional experiments. To recapitulate MLN microenvironment (MLN me), BMDCs were infected as described above in the presence of the supernatants of MLN homogenates obtained from WT or $TNFRp55^{-/-}$ mice on day 14 (MLN me on day 14 [MLN me-day 14]) in a dilution of 1/3 in supplemented RPMI 1640 medium.

Cell preparation and flow cytometry

On days 7, 14, and 21 postinfection (pi), MLN and RLN from C57BL6 WT mice or C57BL6 $TNFRp55^{-/-}$ were collected. The organs were finely cut and digested for 20 min at 37°C in HBSS medium containing collagenase IV (0.5 mg/ml; Sigma-Aldrich, St. Louis, MO) and DNase I (15 μg/ml; Roche Molecular Biochemicals, Mannheim, Germany). Cells were incubated for 15 min at 4°C with anti-mouse CD16/32 (Fc blocking; BD Biosciences, San Diego, CA) and stained with FITC anti-mouse IA/IE (2G9; BD Biosciences), APC anti-mouse CD11c (HL3; BD Biosciences), PE anti-mouse CD11b (M1/70; BD Biosciences), and PerCP Cy5.5 anti-mouse CD103 (2E7; BioLegend) Abs. Data were obtained on a FACSCalibur flow cytometer (BD Biosciences) and analyzed with FlowJo software (Tree Star, Ashland, OR).

For intracellular staining, MLN or RLN cells from naive mice were obtained. These were stimulated with 1 μg/ml of LPS (*Escherichia coli* 0111: B4; Sigma, St. Louis, MO) for 12 h in a humidified atmosphere containing 5% CO_2 at 37°C in supplemented RPMI 1640 medium as described above in the presence of GolgiPlug (BD Biosciences), according to the manufacturer's instructions. Then, the cells were stained with FITC anti-mouse IA/IE and APC anti-mouse CD11c Abs, fixed and permeabilized with BD Fixation and Permeabilization Solution (BD Cytofix/Cytoperm), and after that, they were stained with PE anti-mouse IL-12p40/p70 mAb (clone 15.6; BD Biosciences). Data were obtained with a FACSCalibur cytometer and analyzed using FlowJo software.

Analysis of CCR7 expression

To study CCR7 expression, 2×10^5 BMDCs or MLN DCs were infected as described above. At 24 h pi, the cells were collected and stained with FITC IA/IE, APC CD11c, and PerCpCy5.5 CCR7 (clone 4B12; BioLegend) anti-mouse Abs and analyzed by flow cytometry.

Fingolimod treatment

Fingolimod (FTY720) (Cayman Chemicals, Ann Arbor, MI), was prepared as described by St John et al. (20). FTY720 was dissolved in DMSO in a concentration of 25 mg/ml and stored at −80°C until use. This solution was diluted in sterile PBS containing 2% of hydroxypropyl-β-cyclodextrin (Sigma-Aldrich) for i.p. administration. C57BL6 WT or C57BL6 $TNFRp55^{-/-}$ were infected as described above, and 14 d pi, FTY720 solution was administered via i.p. route in a dosage of 5 mg/kg every 3 d until day 21 pi (Fig. 5A). The control group received PBS.

Assessment of arthritis

Mice were examined daily for the visual appearance of arthritis in peripheral joints, and the arthritis score was calculated until day 21 pi, as described by Banda et al. (21). Clinical severity was classified for each paw, as follows: 0, normal joint; 1, slight inflammation and redness; 2, severe erythematic and swelling affecting the entire paw; and 3, deformed joint paw with ankylosis, joint rigidity, and loss of function. The total score was based on the assessment of all paws, with a maximum score of 12 per animal, as described (9, 10).

Histological study

At day 21, knee joints were dissected. After routine fixation, decalcification, and paraffin embedding, 5-μm-thick sections were cut, stained with H&E, and examined with a light microscope. Photographs were taken using an Olympus BX40 light microscope equipped with Sony SSC-DC5OA camera.

Determination of cytokine production in joints by ELISA

C57BL6 WT or C57BL6 *TNFRp55*$^{-/-}$ were infected and treated with FTY720 as described above. After 21 d pi, joint homogenates were prepared as previously described (10), and IL-12p40 (Mouse IL-12p40 ELISA Set; BD Biosciences) and IFN-γ (BioLegend ELISA Kit; BioLegend, San Diego, CA) were measured according to the manufacturer's instructions. The cytokine concentrations were normalized to the total protein concentrations of the homogenates, which were measured by Qubit Protein Assay Kit (Thermo Fisher Scientific, Waltham, MA).

Statistical analysis

Differences between the groups were tested for significance using the Kruskal–Wallis and Mann–Whitney *U* test, as appropriate. A p value ≤ 0.05 was considered statistically significant. The results are expressed as the mean ± SEM.

Results

TNFRp55 deficiency impact DCs populations in joint-draining lymph nodes (RLN) during arthritis onset

DCs are central players of the immune response that uptake Ags and migrate to draining lymph nodes to prime naive T cells (11). First, we analyzed the recruitment of immune cells in RLN of *TNFRp55*$^{-/-}$ and WT mice after oral *Y. enterocolitica* O:3 infection. We observed that RLN of *TNFRp55*$^{-/-}$ mice were markedly swollen compared with RLN of WT mice (Fig. 1A). This observation correlated with an increase of the total cell number of RLN of *Y. enterocolitica* O:3–infected *TNFRp55*$^{-/-}$ mice (Fig. 1B). These cells were characterized using CD11b and CD11c markers (22). It was detected that all CD11b^{+} populations—CD11c^{+}, CD11c^{int}, and CD11c^{-}—augmented in RLN under TNFR deficiency (Fig. 1C).

Conventional or classical DCs share certain surface markers with other mononuclear phagocytes, namely tissue-resident macrophages, monocytes, and various monocyte-derived cells; however, DCs are characterized as CD11c^{+} cells with a high expression of MHC class II molecules (IA/IE^{high}) (23). Moreover, migration of DCs into initial lymphatic vessels is induced by DC maturation, leading to upregulation of MHC molecules (23). In addition, largely sessile lymph node–resident DCs are present in the T cell area of the draining lymph node (24). Hence, we differentiated migratory (CD11c^{+}IA/IE^{high}) and resident (CD11c^{+}IA/IE^{int}) in the RLN (Fig. 1D, 1E). Recent discoveries have simplified the classification of DC subsets (25). We selected CD11b marker to analyze the two major subpopulations (CD11b^{-} and CD11b^{+} DCs) in migratory and resident DC compartments. In *Y. enterocolitica* O:3–induced ReA model in *TNFRp55*$^{-/-}$ mice, clinical signs of

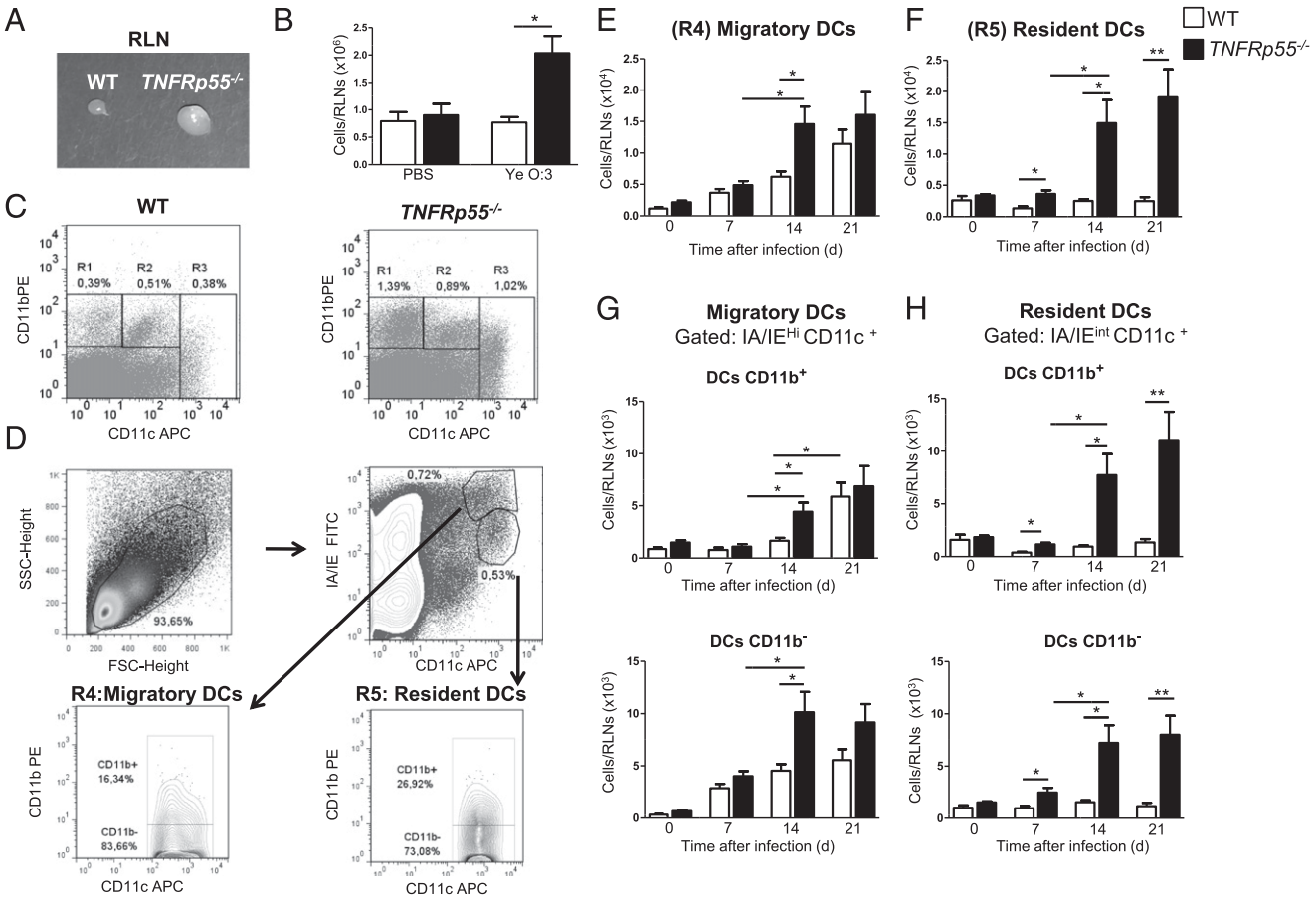

FIGURE 1. Increase of the absolute number of migratory and resident DCs in RLN from *TNFRp55*$^{-/-}$ mice infected with *Y. enterocolitica* O:3. Mice were infected with *Y. enterocolitica* O:3 and euthanized on days 7, 14, and 21 pi. Different populations of cells were analyzed by flow cytometry in RLN. On day 14 after *Y. enterocolitica* infection (arthritis onset), the following is shown: (**A**) RLNs from WT and *TNFRp55*$^{-/-}$ mice; (**B**) total number of cells per RLN; (**C**) inflammatory cells from *TNFRp55*$^{-/-}$ and WT mice (R1: macrophages and neutrophils [CD11b^{+} CD11c^{-}], R2: TNF/inducible NO synthase–producing DCs [CD11b^{+} CD11c^{int})], and R3: conventional DCs [CD11c^{+}]); (**D**–**H**) DCs from RLN [R4: migratory DCs (CD11c^{+} IA/IE^{hi}) (E) and their subpopulations CD11b^{+} or CD11b^{-} DCs (G), and R5: resident DCs (CD11c^{+} IA/IE^{int}) (F) and their subpopulations CD11b$^{+/-}$ DCs (H)]. Data are shown as mean ± SEM (n = 4 per group, representative of at least two independent experiments with similar results). *$p < 0.05$, **$p < 0.01$. *TNFRp55*$^{-/-}$, TNFRp55–deficient mice.

arthritis began to develop on day 14 (arthritis onset) (9, 10). Interestingly, on day 14, the absolute numbers of both migratory and resident DCs were significantly increased in RLN of *TNFRp55*$^{-/-}$ mice compared with the numbers found in RLN of WT mice (Fig. 1E, 1F). Early, on day 7, resident DCs also showed significant augment under TNFRp55 deficiency, and this increase was sustained until day 21 after *Y. enterocolitica* infection. The increase of migratory DCs was delayed in WT mice. In contrast, no modification in the number of resident DCs was detected in RLN of control mice (Fig. 1F). Higher cell numbers of both CD11b^{+} and CD11b^{-} subsets of migratory DCs were found in RLN of *TNFRp55*$^{-/-}$ mice on day 14 (Fig. 1G). In contrast, the CD11b^{-} and CD11b^{+} subpopulations of resident DCs were increased in RLN under TNFRp55 deficiency from day 7 until day 21 (Fig. 1H).

These data demonstrate that TNFRp55 deficiency impacts the infiltration of DCs in joint-draining lymph nodes. The augment of resident DCs of *TNFRp55*$^{-/-}$ mice may indicate early and sustained homing of the precursors of DCs (pre-DCs), via high endothelial venules (HEV), into RLN. Furthermore, marked DC migration through the lymphatics takes place on arthritis onset and is maintained under TNFRp55 deficiency.

DCs augment in MLNs under TNFRp55 deficiency on day 14 after Y. enterocolitica *infection*

A joint–gut axis has been suggested in SpA (12, 26). For T cell priming, after oral Ag administration, DCs transport the Ag from the intestine to MLN. In addition, in *Y. pestis*–lymph node remodeling, infected DCs have been involved in the trafficking of these bacteria through the lymphatic system (20).To know whether joint-draining lymph nodes mirror the changes of DCs of intestinal-draining lymph nodes, we analyzed DCs in MLN. As we detected in RLN, inflamed MLN, as well as more total cells per MLN, were observed in *TNFRp55*$^{-/-}$ mice (Fig. 2A, 2B).

We next investigated the number of migratory and resident DCs in MLN of *TNFRp55*$^{-/-}$and WT mice at different time points after *Y. enterocolitica* O:3 infection. As shown in Fig. 2C and 2D, a peak of both migratory and resident DCs was detected in MLN of *TNFRp55*$^{-/-}$mice on the day of arthritis onset (day 14). Interestingly, migratory DCs significantly dropped in *TNFRp55*$^{-/-}$mice on day 21, reaching levels lower than MLN of WT mice (Fig. 2C). Similarly, resident DCs decreased markedly in their MLN for *TNFRp55*$^{-/-}$ mice on day 21 (Fig. 2D).

When the CD11b^{+} and CD11b^{-} subpopulations were characterized, again both subsets of migratory and resident DCs reached a peak on day 14 in MLN of *TNFRp55*$^{-/-}$ mice (Fig. 2E, 2F). Moreover, CD11b^{-} migratory DCs decreased on day 21 in *TNFRp55*$^{-/-}$ MLN (Fig. 2E). Under gut inflammation, it has been reported that CD11b^{+} DCs have the ability to induce Th17 responses, which have antimicrobial activities in mucosa (11). In the intestine, CD11b^{-} DCs have been described in general terms as exhibiting a special propensity to induce regulatory T cells (11). It is interesting to notice that on day 21, CD11b^{-} DCs were markedly reduced in MLN of *TNFRp55*$^{-/-}$mice (Fig. 2E) in both migratory and resident DC compartments.

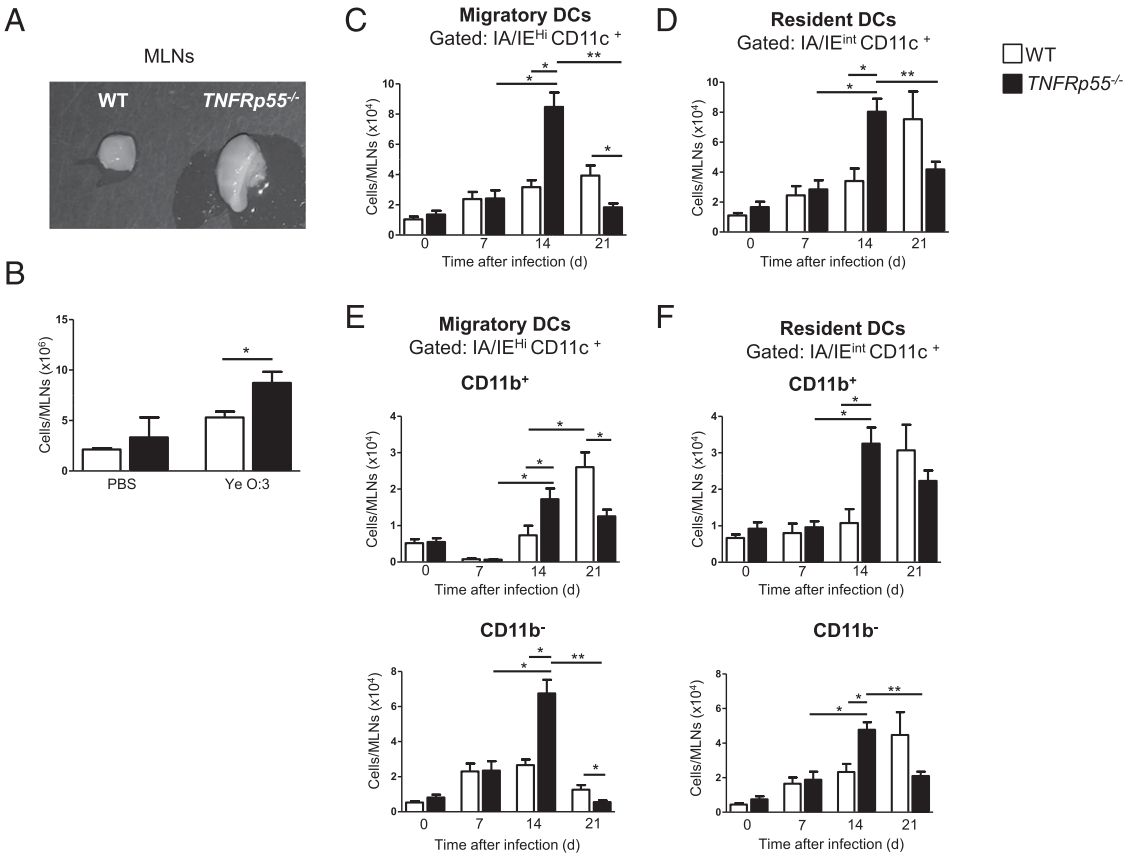

FIGURE 2. Increase of the absolute number of migratory and resident DCs in MLN from *TNRP55*$^{-/-}$ mice infected with *Y. enterocolitica* O:3. DC subpopulations of MLNs from WT and *TNFRp55*$^{-/-}$ mice were analyzed by flow cytometry on days 7, 14, and 21 pi. On day 14 after *Y. enterocolitica* infection (arthritis onset), the following is shown: (**A**) MLNs from WT and *TNFRp55*$^{-/-}$ mice; (**B**) total number of cells per MLNs; and DCs from MLNs: migratory DCs (CD11c^{+} IA/IE^{hi}) (**C**) and their subpopulations CD11b^{+} or CD11b^{-} DCs (**E**), and resident DCs (CD11c^{+} IA/IE^{int}) (**D**) and their subpopulations CD11b$^{+/-}$ DCs (**F**). Data are shown as mean ± SEM ($n = 4$ per group, representative of at least two independent experiments with similar results). *$p < 0.05$, **$p < 0.01$. *TNFRp55*$^{-/-}$, TNFRp55–deficient mice.

Overall, these results demonstrate changes in the number of DCs in MLN of *TNFRp55*$^{-/-}$ mice. Considering that on day 14, the changes of migratory DCs in MLN mirror those observed in RLN, we suggest a DC trafficking from MLN to RLN. Migratory DCs peaked on arthritis onset in MLN under TNFRp55 deficiency. On day 21, these cells decreased only in *TNFRp55*$^{-/-}$mice. Therefore, it could be suggested that TNFRp55 signaling controls the migration of DCs to MLN, orchestrates a regulatory response in mucosa, and consequently contributes to avoid *Y. enterocolitica*–induced ReA development.

Migratory DCs of MLN produce IL-12/23p40, and Y. enterocolitica *O:3 infection induces CCR7 expression in DCs*

In previous studies, we have demonstrated increased levels of IL-12/23p40 in *Y. enterocolitica*–induced ReA in *TNFRp55*$^{-/-}$ mice (10). Recently, we have confirmed that DCs participate in this IL-12/23p40 overproduction (16). Therefore, we evaluated whether migratory or resident DCs of MLN of *TNFRp55*$^{-/-}$ mice are the main source of IL-12/23p40. To explore intracellular IL-12/23p40 production in the early hours, cells from MLN or RLN of naive *TNFRp55*$^{-/-}$ and WT mice were LPS stimulated for 12 h, and then the frequencies of IL-12/23p40^{+} migratory or resident DCs were evaluated. We found a higher frequency of IL-12/23p40^{+} migratory DCs in *TNFRp55*$^{-/-}$ MLN when compared with WT MLN (Fig. 3A). In contrast, neither migratory nor resident DCs from naive *TNFRp55*$^{-/-}$ RLN showed differences when compared with DCs from WT RLN (Fig. 3B).

The chemokine receptor CCR7 is essentially involved in the migration of DCs toward or into lymphatics (27). Upregulation of CCR7 expression on DCs is induced by early recognition of the pathogen by these cells (11). Hence, BMDCs were obtained and infected with *Y. enterocolitica* O:3 at moi 10:1 for 1 h. After killing extracellular bacteria, BMDCs were cultured for 24 h, and the CCR7 expression was analyzed by flow cytometry. Uninfected *TNFRp55*$^{-/-}$ BMDCs expressed higher levels of CCR7 than uninfected WT BMDCs (Fig. 3C). *Y. enterocolitica* O:3 infection induced an increase of CCR7 expression in BMDCs, which was significantly higher in *TNFRp55*$^{-/-}$ BMDCs (Fig. 3C). To recapitulate the MLN me-day 14 in BMDCs, these cells were infected in the presence of supernatants of homogenates of MLN obtained from WT or *TNFRp55*$^{-/-}$ on day 14. As expected, significant higher CCR7 expression was detected on *Y. enterocolitica*–infected BMDCs from *TNFRp55*$^{-/-}$ mice in knockout MLN me-day 14 compared with the same cells in WT MLN me-day 14 (Fig. 3C). Interestingly, *Y. enterocolitica*–infected BMDCs from WT mice in knockout MLN me-day 14 increased CCR7 expression, reaching the same level of *Y. enterocolitica*–infected *TNFRp55*$^{-/-}$ BMDCs (Fig. 3C).

These data suggest that migratory DCs from MLN are an essential source of IL-12/23p40 in *TNFRp55*$^{-/-}$ mice. RLN could depend on DC migration from MLN. Furthermore, after *Y. enterocolitica* O:3 infection, TNFRp55 deficiency may promote DC migration into lymph nodes via lymphatics by inducing the CCR7 expression on DC.

Intestinal DC subsets reach joint-draining lymph nodes under TNFRp55 deficiency

Intestinal lamina propria DCs have the capacity to migrate in afferent lymphs to MLN (11). Although early work assumed that intestinal DCs comprised a homogeneous population of CD103^{+} cells, most recent studies have divided them on the basis of CD103

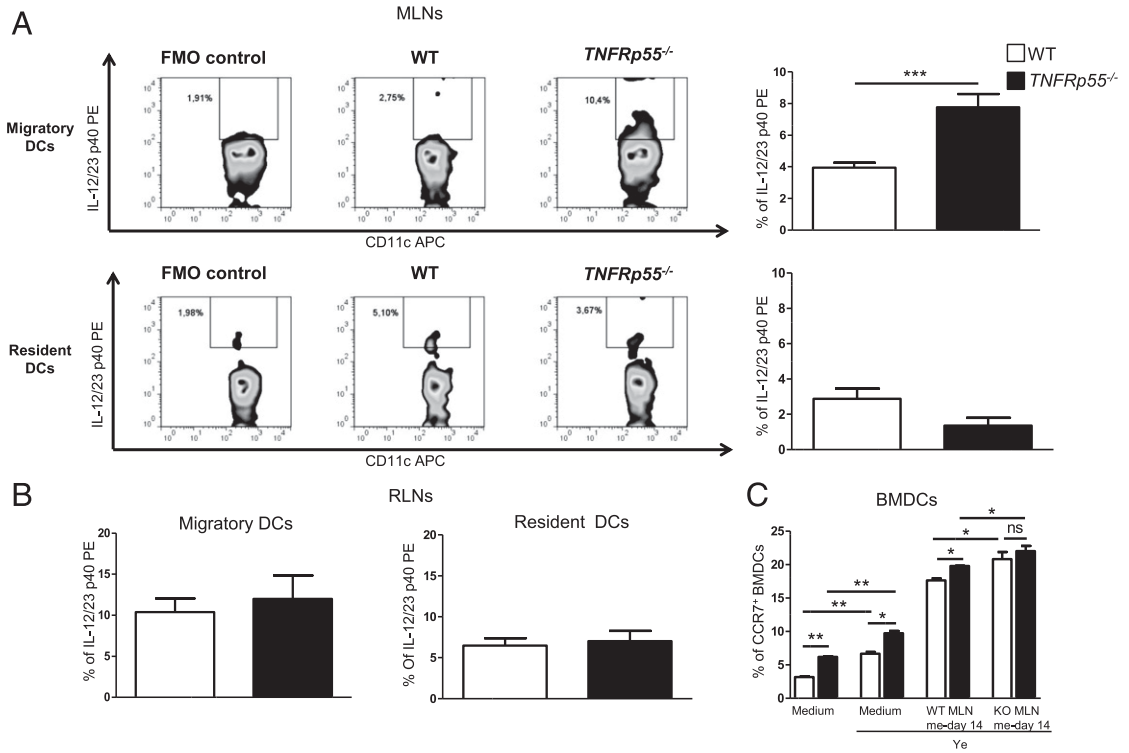

FIGURE 3. In vitro production of IL-12/23p40 by MLN migratory DCs and induction CCR7 expression in BMDCs by *Y. enterocolitica* O:3 infection. MLN (**A**) or RLN (**B**) cells from naive mice were stimulated with 1 μg/ml of LPS, and intracellular IL-12/23p40 was analyzed by flow cytometry. (**C**) BMDCs in the absence or presence of MLN me-day 14 were infected in vitro with *Y. enterocolitica* O:3 at moi 10:1 for 1 h, and CCR7 expression was analyzed by flow cytometry. Data are shown as mean ± SEM [n = 3–4 per group, pooled of two independent experiments in (A) and (B), and representative of two independent experiments in (C)]. *$p < 0.05$, **$p < 0.01$, ***$p < 0.001$. FMO, fluorescence minus one; LPS, LPS of *E. coli*; *TNFRp55*$^{-/-}$, TNFRp55–deficient mice.

and CD11b expressions (28, 29). To track intestinal DC migration to RLN, gastrointestinal infection with *Y. enterocolitica* O:3–GFP was performed, and GFP$^+$ CD103$^+$ DCs were examined in RLN early pi (day 5) because bacteria are not found in the joint and RLN once ReA is detected (Fig. 4A). Furthermore, to analyze DC migration between MLN and RLN on arthritis onset, we evaluated the major subsets of the migratory DC compartment of MLN in RLN on day 14: CD103$^+$CD11b$^-$, CD103$^-$CD11b$^+$, and CD103$^+$CD11b$^+$. Five days after oral *Y. enterocolitica* O:3–GFP infection, GFP$^+$ intestinal DC subpopulations were found in RLN of both WT and *TNFRp55*$^{-/-}$ mice (Fig. 4A). In contrast with WT mice, *TNFRp55*$^{-/-}$ mice presented a marked increase of the three major intestinal DC subsets in their RLN on arthritis onset (Fig. 4B–D).

Therefore, early pi, intestinal DCs travels with *Y. enterocolitica* O:3 to RLN. TNFRp55 deficiency enhances the recruitment of intestinal DCs into RLN, which supports the connection between intestinal and joint-draining lymph node. This may sustain *Y. enterocolitica* O:3–induced ReA in *TNFRp55*$^{-/-}$ mice.

Inhibition of DC migration toward RLN by the administration of FTY720 ameliorates Y. enterocolitica *O:3–induced ReA*

FTY720 is an immune modulator derived from myriocin that inhibits the functions of sphingosine-1 phosphate, a potent bioactive sphingolipid metabolite that regulates many cellular processes, including cell migration (30, 31). In previous studies, it has been demonstrated that FTY720 suppresses the development of collagen-induced arthritis by interfering with DC migration (30). Therefore, we assessed the effect of blocking DC migration by FTY720 on *Y. enterocolitica* O:3–induced ReA in *TNFRp55*$^{-/-}$ mice. Because 50–60% of these knockout mice died because of *Y. enterocolitica* O:3 infection (9, 10), we started the FTY720 treatment in the surviving mice since day 14 pi every 3 d until day 21 (Fig. 5A). All the studies were performed on day 21 pi. We first examined DC populations in RLN and observed a slight reduction of the absolute number of total migratory DCs in FTY720-treated *TNFRp55*$^{-/-}$ mice ($p = 0.06$) (Fig. 5B). Although this reduction is not significant, both CD11b$^+$ and CD11b$^-$ subsets of migratory DCs exhibited a significantly lower absolute number in RLN of *TNFRp55*$^{-/-}$ mice after FTY720 treatment (Fig. 5C). In addition, FTY720 treatment significantly decreased the absolute number of total resident DCs and their subpopulation CD11b$^+$ and CD11b$^-$ in RLN of *TNFRp55*$^{-/-}$ mice (Fig. 5D, 5E). Furthermore, FTY720 treatment reduced the clinical score of arthritis in *TNFRp55*$^{-/-}$ mice (Fig. 6A). In agreement with these results, histological examination revealed that FTY720 treatment diminished synovial hyperplasia, cartilage erosion, and bone loss when compared with nontreated *TNFRp55*$^{-/-}$ mice (Fig. 6B).

It has been reported that CD11b$^-$ DCs are the primary subset that produces more IL-12, which promotes Th1 response under proinflammatory conditions (25). We detected a lower number of migratory CD11b$^-$ DCs in RLN of FTY720-treated *TNFRp55*$^{-/-}$ mice (Fig. 5C). Moreover, IL-12/23p40 and IFN-γ are key cytokines in *Y. enterocolitica* O:3–induced ReA in *TNFRp55*$^{-/-}$ mice (10). Hence, we investigated the levels of these two proinflammatory cytokines in joint homogenates. High concentration of IL-12/23p40 and IFN-γ were detected in *Y. enterocolitica* O:3–infected *TNFRp55*$^{-/-}$ mice when compared with *Y. enterocolitica* O:3–infected WT mice. On the contrary, both cytokines (Fig. 7A, 7B) significantly reduced to the levels found in the control mice in the joints of FTY720-treated *TNFRp55*$^{-/-}$ mice.

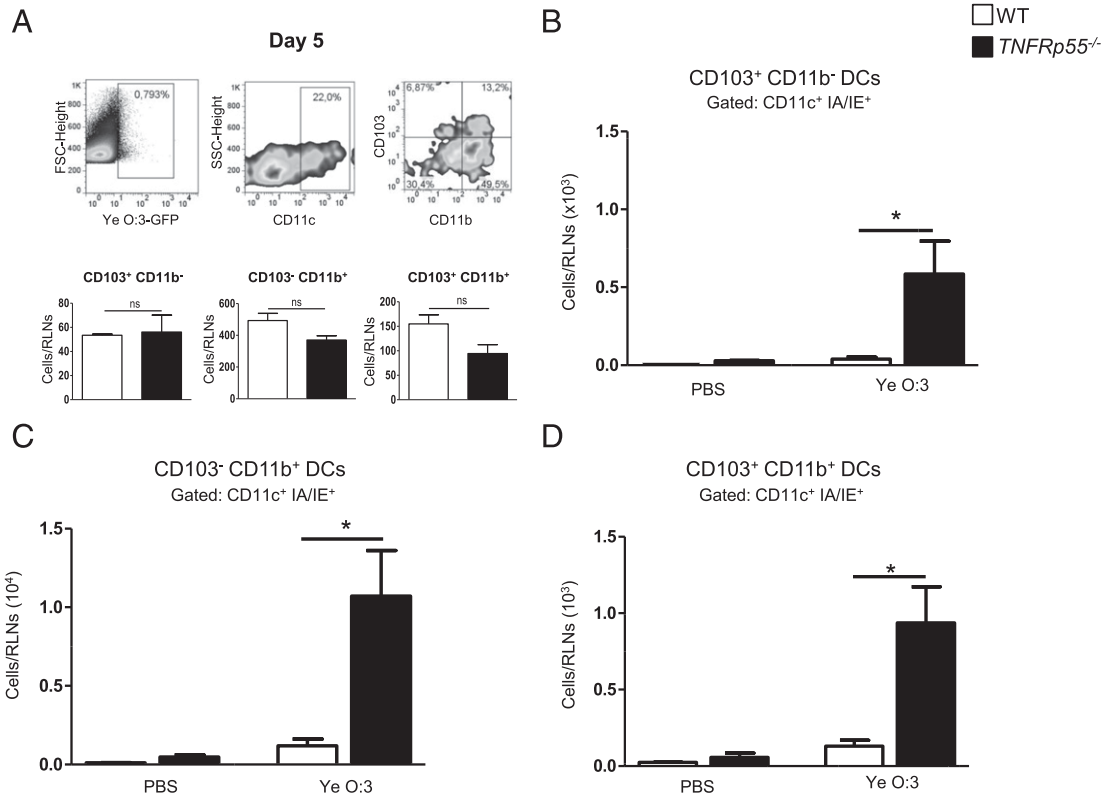

FIGURE 4. *TNFRp55*$^{-/-}$ mice infected with *Y. enterocolitica* O:3 for 14 d present an increase of intestinal DC subsets in RLN. (**A**) Intestinal GFP$^+$ DC subsets reach RLN of WT and *TNFRp55*$^{-/-}$ mice 5 d after *Y. enterocolitica* O:3–GFP infection. On arthritis onset (day 14), intestinal DC subsets accumulate in *TNFRp55*$^{-/-}$ mice: (**B**) CD103$^+$CD11b$^-$, (**C**) CD103$^-$CD11b$^+$, and (**D**) CD103$^+$CD11b$^+$. Data are shown as mean ± SEM ($n = 4$ per group, representative of two independent experiments with similar results). *$p < 0.05$. ns, not significant.

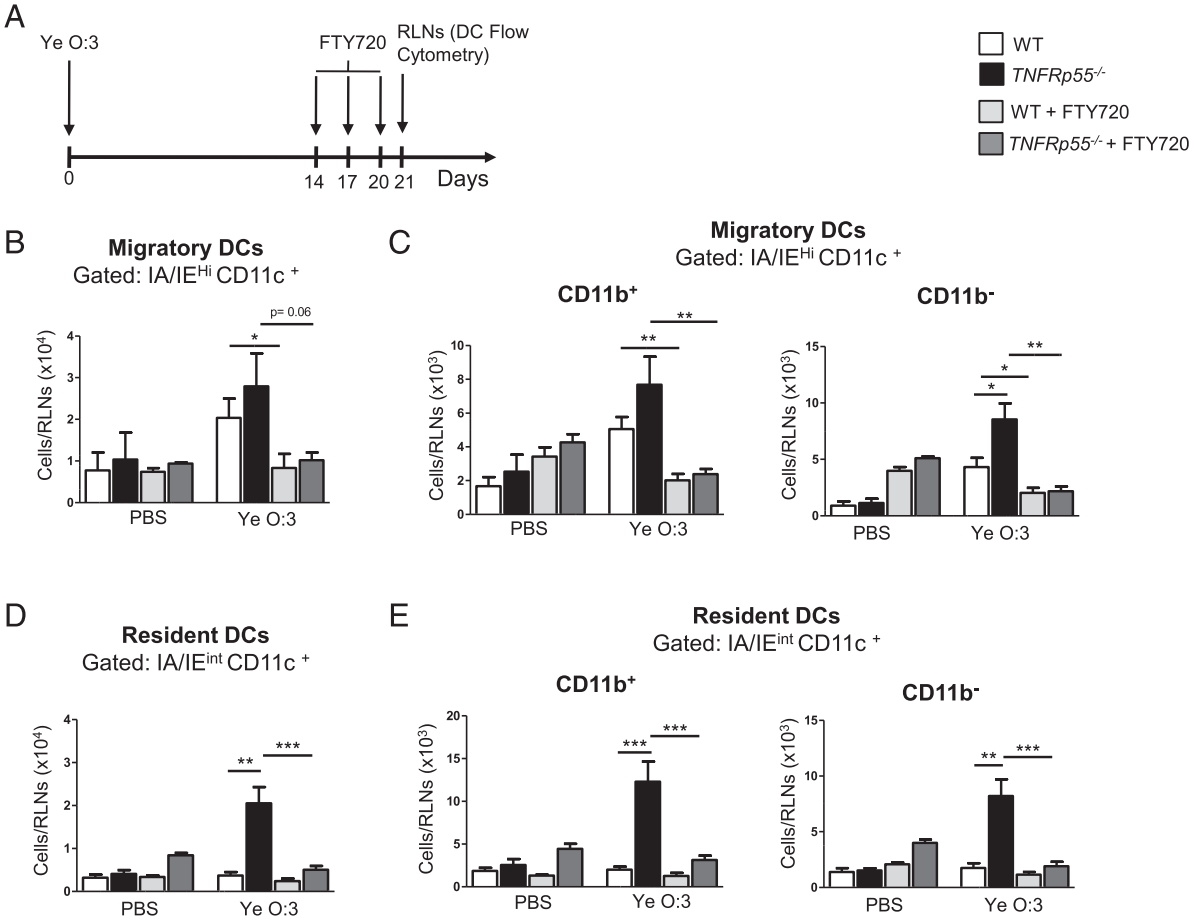

FIGURE 5. FTY720 treatment reduces the absolute number of DCs and its subpopulations in RLNs from *TNFRp55*$^{-/-}$ mice infected with *Y. enterocolitica* O:3. (**A**) WT and *TNFRp55*$^{-/-}$ mice infected with *Y. enterocolitica* O:3 for 14 d were treated i.p. with FTY720 every 3 d until day 21 pi. Then, migratory and resident DCs were analyzed by flow cytometry in RLNs. (**B**) Absolute number of migratory DCs and their subpopulations: (**C**) CD11b^{+} or CD11b^{-}. (**D**) Absolute number of resident DCs and their subpopulations: (**E**) CD11b^{+} or CD11b. Data are shown as mean ± SEM (n = 4 per group, data pooled of two independent experiments). *$p < 0.05$, **$p < 0.01$, ***$p < 0.001$.

CCR7 is a crucial chemokine receptor for DC migration. Therefore, we explored whether CCR7 is associated with the mechanisms underlying the FTY720 inhibitory effect on DC migration. We performed in vitro experiments to analyze the effect of FTY720 on the expression of CCR7 onto the DC membrane. As shown in Fig. 7C and 7D, FTY720 treatment downregulated CCR7 expression on *Y. enterocolitica* O:3–infected BMDCs or purified MLN DCs.

Our results demonstrate that CCR7-mediated DC migration into RLN plays an important role in the pathogenesis of *Y. enterocolitica* O:3–induced ReA under TNFRp55 deficiency.

Discussion

The relationship between gut and joint is clear in ReA because this type of SpA develops from an antecedent gastrointestinal infection (12). However, how this immunopathogenic intestine–joint connection operates in this disease, to the best of our knowledge, has not been thoroughly described. DCs are powerful APCs whose appropriate localization is essential in the initiation or regulation of the immune response (27). Therefore, DC migration has been demonstrated to be fundamental in the maintenance of the tissue homeostasis and also of different pathogenic conditions (11, 27). Moreover, infected DCs are involved in the trafficking of *Y. pestis* among lymph nodes through the lymphatic system (20). In a previous study, we showed a pathogenic role of DCs as the main cellular source of IL-12/23p40 in *Y. enterocolitica* O:3–induced ReA in *TNFRp55*$^{-/-}$mice (16). In the present work, we examine DCs in RLN and MLN to investigate the gut–joint association in this murine model of ReA.

We initially observed inflammation and an increased absolute number of total cells in RLN of *TNFRp55*$^{-/-}$ mice on day 14 after *Y. enterocolitica* infection. This may reflect an influx of proinflammatory cells to RLN on the day that we previously reported as the day of arthritis onset (10). The ability to migrate to draining lymph nodes is a key characteristic of DCs. After sampling the foreign Ag, an intrinsic program induces DC maturation, leading to upregulation of MHC class II (11). We found migratory DCs (CD11c^{+}IA/IE^{high}) in RLN of the mice, indicating that DCs travel from the intestine to these lymph nodes. We detected a migration of DCs in *TNFRp55*$^{-/-}$ RLN (day 14), which was earlier than in WT RLN (day 21). In fact, it has been reported that TNF through TNFRp55 and TNFRp75 regulates DC maturation and survival (32). In addition, DCs have been shown to be important host cells for the dissemination of various pathogens (33). Although no bacteria are present in the joints of *TNFRp55*$^{-/-}$ mice with ReA (9), we detected that DCs traffic *Y. enterocolitica* O:3–GFP from the intestine to RLN early pi. Therefore, we suppose that DCs traffic bacterial Ags from the intestine to RLN, which is significant under TNFRp55 deficiency. However, whether *Y. enterocolitica* Ags are internalized in migratory DCs of RLN remains to be addressed. A second pathway of Ag delivery is mediated by resident DCs that present soluble Ags and enter via the afferent

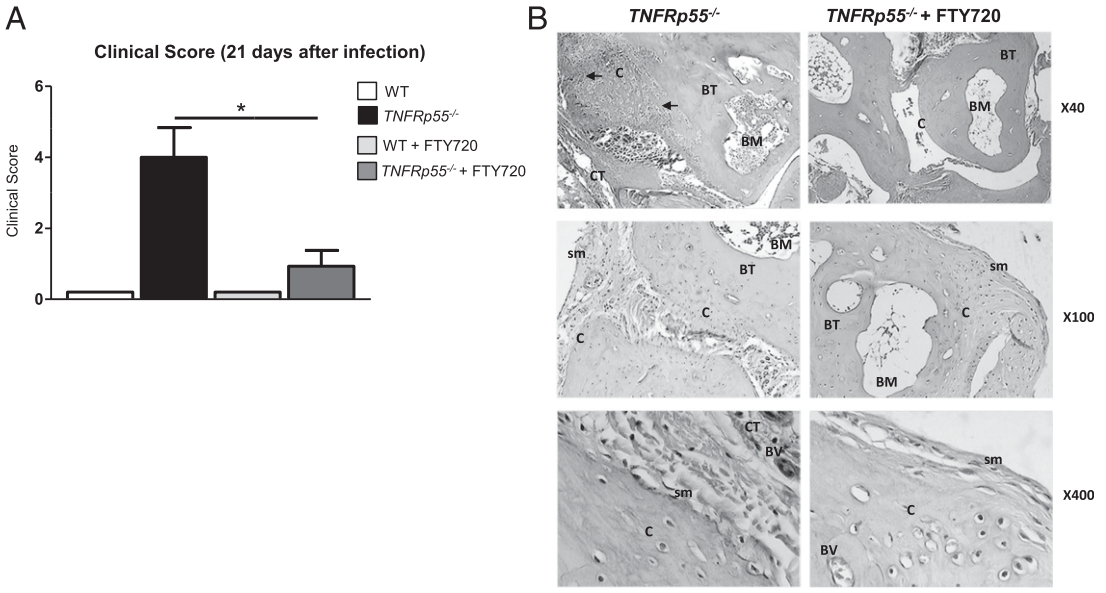

FIGURE 6. FTY720 treatment ameliorates *Y. enterocolitica* O:3–induced ReA. WT or *TNFRp55*$^{-/-}$ mice were infected orogastrically with *Y. enterocolitica* O:3. After 14 d, FTY720 was administrated i.p. every 3 d until 21 d pi. (**A**) The different groups of mice were monitored for arthritis clinical severity at day 21 pi. The clinical score was calculated as described in *Materials and Methods*. Data are shown as mean ± SEM ($n = 6$ per group, data pooled from three independent experiments). *$p < 0.05$. (**B**) Histopathological examination of representative joints of untreated *TNFRp55*$^{-/-}$ and FTY720-treated *TNFRp55*$^{-/-}$ mice on day 21 pi. Arrows indicate chondrocyte proliferation. C, chondrocytes; BM, bone marrow; BT, bone tissue; BV, blood vessel; CT, connective tissue; sm, synovial membrane.

lymphatics in the T cell area of the draining lymph node. This happens before there is any detectable DC migration from the periphery (34). Accordingly, resident DCs increased in *TNFRp55*$^{-/-}$ RLN from day 7–21 after *Y. enterocolitica* infection, but no changes in this DC population was detected in WT RLN. Because *TNFRp55*$^{-/-}$ mice are susceptible to *Y. enterocolitica* infection (9), it is probable that from blood, pre-DCs gain access to lymph nodes via HEVs early pi, and they increase the resident DC network. In addition, *TNFRp55*$^{-/-}$ mice exhibit a selective defect in the development of PP (35). As a result, more intestinal soluble Ags may

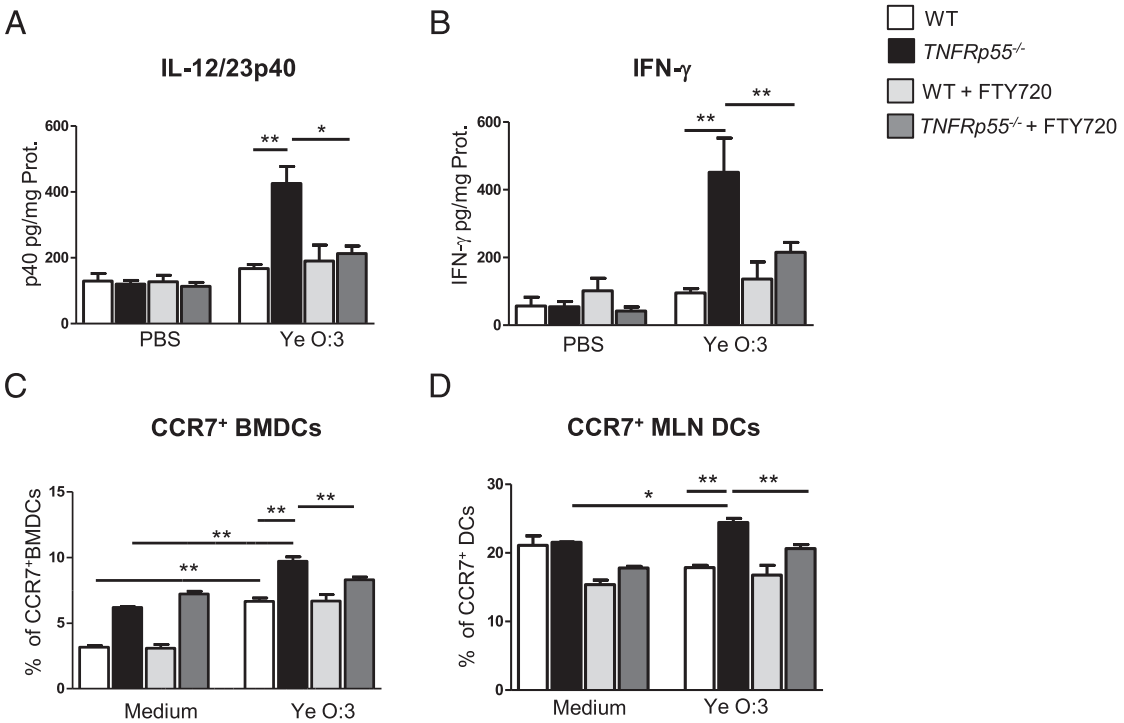

FIGURE 7. FTY720 treatment reduces IL-12 and IFN-γ in *TNFRp55*$^{-/-}$–infected mice and CCR7 expression in *TNFRp55*$^{-/-}$ BMDCs and MLN DCs after in vitro infection. (**A** and **B**) WT and *TNFRp55*$^{-/-}$ mice infected with *Y. enterocolitica* O:3 for 14 d were treated with FTY720 every 3 d until day 21 pi. Later, IL-12/23p40 (A) and IFN-γ (B) were measured in joint homogenates by ELISA. Data are shown as mean ± SEM ($n = 4$ per group, data pooled from three independent experiments). *$p < 0.05$, **$p < 0.01$. BMDCs (**C**) or MLN DCs (**D**) from WT or *TNFRP55*$^{-/-}$ mice were infected with *Y. enterocolitica* O:3 at moi 10:1 for 1 h. Then, BMDCs were cultured by an additional 24 h, and CCR7 expression was measured by flow cytometry. Data are shown as mean ± SEM ($n = 3$) and are representative of two independent experiments with similar results. *$p < 0.05$, **$p < 0.01$.

reach RLN and then promote resident DC differentiation. Detailed analysis of the $CD11b^+$ and $CD11b^-$ subsets of both migratory and resident DC compartments revealed that both subtypes increased in *TNFRp55*$^{-/-}$ RLN. Therefore, under TNFRp55 deficiency, both resident DC subsets may interact with the T cells retained in the RLN and cooperate to their expansion and differentiation.

It has been recently demonstrated that the transport of *Y. enterocolitica* to MLN is dependent on CCR7-expresing CD103 DCs (6). Similarly, other reports showed that after *Salmonella* oral infection, migratory DCs are the only immune cells that can carry the viable bacteria from the site of infection through migration in lymph to the MLN (36). Furthermore, acute mesenteric lymphadenitis is one of the most characteristic forms of *Y. enterocolitica* infection in humans (37), and clinical cases caused by these bacteria have identified the MLN as a primary site of infection (38). Indeed, we also found inflammation and cellular influx in MLN. A peak of both migratory and resident DCs was observed in *TNFRp55*$^{-/-}$ MLN on arthritis onset (day 14), mirroring the changes of cells in RLN. In contrast with MLN of WT mice, MLN of *TNFRp55*$^{-/-}$ mice showed a transient increase of migratory and resident DCs on day 14, but a considerable increase of migratory $CD11b^+$ DCs was detected in MLN of WT mice on day 21. Following activation, this subset has been described to induce Th17 cells, which promotes protective responses against mucosal infection (11). This evidence is in agreement with our previous report, which showed a marked increase of IL-17 in MLN of WT mice on 21 d after *Y. enterocolitica* infection (10). Interestingly, $CD11b^-$ DCs reduced in MLN of *TNFRp55*$^{-/-}$ mice in both migratory and resident DC compartments (Fig. 2E, 2F). This DC subset has the ability to induce regulatory T cells (11, 29). Coincidentally, in our prior studies, both TGF-β and IL-10, which are critical immunosuppressive cytokines produced by regulatory T cells, were detected augmented in MLNs of WT mice only 21 d pi (10, 39). Therefore, DCs of MLN may promote regulatory mechanisms presumably mediated by TNFRp55, which is crucial for controlling ReA development.

We have previously reported data that strongly support a role of the TNFRp55 pathway in controlling IL-12/23p40 (16). A cross-talk between TNFRp55 and TLR4 signaling has been identified, and the candidate protein A20 has been associated as a negative regulator of the core cross-talk element TNFR-associated factor 6 (40). Thus, in a mouse model in which $CD11c^+$ cells, including DCs, lack expression of A20, the *A20*$^{-/-}$ DCs produce a higher concentration of IL-12 when they are stimulated with bacterial products (41). Interestingly, these mice spontaneously developed lymphocyte-dependent colitis, seronegative ankylosing arthritis, and enthesitis (41). Hence, DCs may drive *Y. enterocolitica*–induced ReA in *TNFRp55*$^{-/-}$ mice through their overproduction of IL-12/23p40. When we stimulated naive DCs from MLN with LPS in vitro, we observed that migratory DCs were the source of IL-12/23p40 and that the frequency of IL-12/23p40$^+$ migratory DCs was higher in cells of *TNFRp55*$^{-/-}$ MLN. In contrast, naive DCs from *TNFRp55*$^{-/-}$ RLN did not secrete IL-12/23p40 after in vitro LPS stimulation, supporting the requirement of MLN–RLN connection. The MLN and RLN link is also evident because the major subsets of the migratory DC compartment of MLN ($CD103^+CD11b^-$, $CD103^-CD11b^+$, and $CD103^+CD11b^+$) (28) were found in *TNFRp55*$^{-/-}$ RLN on day 14. Moreover, when migration was tracked in the *Y. enterocolitica*–GFP infection, GFP^+CD103^+ DCs were found in *TNFRp55*$^{-/-}$ RLN on day 5 pi. Therefore, it is tempting to speculate that DCs travel via lymph from MLN to RLN. Thus, DCs have been isolated from the efferent lymphs (42). Furthermore, *Y. pestis* disseminate intracellularly in DCs beyond draining lymph nodes to downstream lymph nodes (20). These cells may exit via efferent lymphs and travel through the lymphatic vasculature to drain to higher-order lymph nodes (20). Furthermore, we could show that both *TNFRp55*$^{-/-}$ BMDCs in MLN environment (Fig. 3C) and DCs isolated from *TNFRp55*$^{-/-}$ MLN (Fig. 7D) upregulated CCR7 under in vitro *Y. enterocolitica* O:3 infection. This chemokine receptor, expressed on migrating DCs, interacts with its ligand CCL21, which is found on lymphatic endothelial cells. This CCR7–CCL21 axis guides DC entry to afferent lymphatic vessels and through stromal networks into the T cell–rich paracortex in lymph nodes (27, 43). Therefore, our results support the hypothesis that TNFRp55 deficiency promotes enhanced CCR7-dependent DC migration into lymph nodes. Based on our data, we favor the notion that, at least in our model of *TNFRp55*$^{-/-}$ mice, DCs participate in ReA pathogenicity, connecting intestine and joint-draining lymph nodes and secreting IL-12/23p40.

Finally, we abrogate DC migration by FTY720 treatment evidenced by the reduction of migratory DC subsets in *TNFRp55*$^{-/-}$ RLN. This was associated with the decrease of IL-12/23p40 and IFN-γ in the joints of FTY720-treated *TNFRp55*$^{-/-}$ mice. In the same line, $CD11b^-$ DC subpopulation has been demonstrated to produce IL-12 and therefore promotes Th1 response under proinflammatory conditions (25). Similarly, FTY720 treatment decreased the production of IL-12 and IL-23 in LPS-stimulated DCs via the common subunit p40 as well as in the cross-talk with activated keratinocytes (44). In addition, FTY720 treatment reduced the severity of the ReA in *TNFRp55*$^{-/-}$ mice. Additionally, we found that FTY720 treatment reduced the total resident DCs and their subpopulation $CD11b^+$ and $CD11b^-$ in RLN of *TNFRp55*$^{-/-}$ mice. The factors that participate in the entry of the pre-DCs via HEVs from blood into the network of resident DCs in lymph nodes are not yet resolved. However, CCR7 internalization and/or desensitization might be involved (45). Therefore, we cannot exclude the contribution of resident DCs for *Y. enterocolitica*–induced ReA development under TNFRp55 deficiency. Consistent with our results, FTY720 has modulated DC migration to local lymph nodes in several mouse disease models, alleviating the clinical symptoms of the diseases (30, 46–48). In addition, we have shown that the mechanism underlying the effect of FTY720 on DC trafficking involves CCR7 expression because FTY720 treatment of *Y. enterocolitica*–infected *TNFRp55*$^{-/-}$ BMDCs and purified MLN DCs decreased the expression of this chemokine receptor. This mechanism fully concurs with the published findings obtained in different settings (30, 47–49).

In conclusion, we provide evidence that DCs mediate the link between intestine and joints in ReA induced by oral *Y. enterocolitica* O:3 infection under TNFRp55 deficiency. Furthermore, our data indicate that FTY720 treatment blocks DC trafficking to local lymph nodes, which may represent a potential strategy to treat ReA induced by intestinal infection.

Acknowledgments

We acknowledge Gabinete de Asesoramiento en Escritura Científica en Inglés of Universidad Nacional de San Luis for improvement of the language of the manuscript. Moreover, the authors thank Marisol Velazquez for the preparation of *Y. enterocolitica* O:3–GFP.

Disclosures

The authors have no financial conflicts of interest.

References

1. Generali, E., T. Bose, C. Selmi, J. W. Voncken, and J. G. M. C. Damoiseaux. 2018. Nature versus nurture in the spectrum of rheumatic diseases: classification

of spondyloarthritis as autoimmune or autoinflammatory. *Autoimmun. Rev.* 17: 935–941.
2. Selmi, C., and M. E. Gershwin. 2014. Diagnosis and classification of reactive arthritis. *Autoimmun. Rev.* 13: 546–549.
3. Taams, L. S., K. J. A. Steel, U. Srenathan, L. A. Burns, and B. W. Kirkham. 2018. IL-17 in the immunopathogenesis of spondyloarthritis. *Nat. Rev. Rheumatol.* 14: 453–466.
4. Tuompo, R., T. Hannu, E. Huovinen, L. Sihvonen, A. Siitonen, and M. Leirisalo-Repo. 2017. *Yersinia enterocolitica* biotype 1A: a possible new trigger of reactive arthritis. *Rheumatol. Int.* 37: 1863–1869.
5. Bancerz-Kisiel, A., M. Pieczywek, P. Łada, and W. Szweda. 2018. The most important virulence markers of *Yersinia enterocolitica* and their role during infection. *Genes (Basel)* 9: E235.
6. Drechsler-Hake, D., H. Alamir, J. Hahn, M. Günter, S. Wagner, M. Schütz, E. Bohn, K. Schenke-Layland, F. Pisano, P. Dersch, et al. 2016. Mononuclear phagocytes contribute to intestinal invasion and dissemination of Yersinia enterocolitica. *Int. J. Med. Microbiol.* 306: 357–366.
7. Uliczka, F., F. Pisano, J. Schaake, T. Stolz, M. Rohde, A. Fruth, E. Strauch, M. Skurnik, J. Batzilla, A. Rakin, et al. 2011. Unique cell adhesion and invasion properties of *Yersinia enterocolitica* O:3, the most frequent cause of human Yersiniosis. *PLoS Pathog.* 7: e1002117.
8. Steeland, S., C. Libert, and R. E. Vandenbroucke. 2018. A new venue of TNF targeting. *Int. J. Mol. Sci.* 19: E1442.
9. Di Genaro, M. S., D. E. Cargnelutti, J. R. Eliçabe, M. G. Lacoste, S. Valdez, N. Gómez, and A. M. de Guzmán. 2007. Role of TNFRp55 in *Yersinia enterocolitica* O:3-induced arthritis: triggering bacterial antigens and articular immune response. *Rheumatology (Oxford)* 46: 590–596.
10. Eliçabe, R. J., E. Cargnelutti, M. I. Serer, P. W. Stege, S. R. Valdez, M. A. Toscano, G. A. Rabinovich, and M. S. Di Genaro. 2010. Lack of TNFR p55 results in heightened expression of IFN-γ and IL-17 during the development of reactive arthritis. *J. Immunol.* 185: 4485–4495.
11. Worbs, T., S. I. Hammerschmidt, and R. Förster. 2017. Dendritic cell migration in health and disease. *Nat. Rev. Immunol.* 17: 30–48.
12. Asquith, M., D. Elewaut, P. Lin, and J. T. Rosenbaum. 2014. The role of the gut and microbes in the pathogenesis of spondyloarthritis. *Best Pract. Res. Clin. Rheumatol.* 28: 687–702.
13. Merilahti-Palo, R., K. O. Söderström, R. Lahesmaa-Rantala, K. Granfors, and A. Toivanen. 1991. Bacterial antigens in synovial biopsy specimens in yersinia triggered reactive arthritis. *Ann. Rheum. Dis.* 50: 87–90.
14. Kontoyiannis, D., M. Pasparakis, T. T. Pizarro, F. Cominelli, and G. Kollias. 1999. Impaired on/off regulation of TNF biosynthesis in mice lacking TNF AU-rich elements: implications for joint and gut-associated immunopathologies. *Immunity* 10: 387–398.
15. Rescigno, M., and A. Di Sabatino. 2009. Dendritic cells in intestinal homeostasis and disease. *J. Clin. Invest.* 119: 2441–2450.
16. Mayordomo, A. C., J. E. Silva, C. V. Gorlino, J. L. Arias, W. Berón, and M. S. Di Genaro. 2018. IL-12/23p40 overproduction by dendritic cells leads to an increased Th1 and Th17 polarization in a model of *Yersinia enterocolitica*-induced reactive arthritis in *TNFRp55*$^{-/-}$ mice. *PLoS One* 13: e0193573.
17. Oellerich, M. F., C. A. Jacobi, S. Freund, K. Niedung, A. Bach, J. Heesemann, and K. Trülzsch. 2007. *Yersinia enterocolitica* infection of mice reveals clonal invasion and abscess formation. *Infect. Immun.* 75: 3802–3811.
18. Gensberger, E. T., and T. Kostić. 2017. Green fluorescent protein labeling of food pathogens *Yersinia enterocolitica* and *Yersinia pseudotuberculosis*. *J. Microbiol. Methods* 132: 21–26.
19. Lutz, M. B., N. Kukutsch, A. L. Ogilvie, S. Rössner, F. Koch, N. Romani, and G. Schuler. 1999. An advanced culture method for generating large quantities of highly pure dendritic cells from mouse bone marrow. *J. Immunol. Methods* 223: 77–92.
20. St John, A. L., W. X. G. Ang, M. N. Huang, C. A. Kunder, E. W. Chan, M. D. Gunn, and S. N. Abraham. 2014. S1P-dependent trafficking of intracellular *yersinia pestis* through lymph nodes establishes Buboes and systemic infection. *Immunity* 41: 440–450.
21. Banda, N. K., A. Vondracek, D. Kraus, C. A. Dinarello, S. H. Kim, A. Bendele, G. Senaldi, and W. P. Arend. 2003. Mechanisms of inhibition of collagen-induced arthritis by murine IL-18 binding protein. *J. Immunol.* 170: 2100–2105.
22. Sundquist, M., and M. J. Wick. 2009. *Salmonella* induces death of CD8alpha(+) dendritic cells but not CD11c(int)CD11b(+) inflammatory cells i*n vivo* via MyD88 and TNFR1. *J. Leukoc. Biol.* 85: 225–234.
23. Merad, M., P. Sathe, J. Helft, J. Miller, and A. Mortha. 2013. The dendritic cell lineage: ontogeny and function of dendritic cells and their subsets in the steady state and the inflamed setting. *Annu. Rev. Immunol.* 31: 563–604.
24. Sixt, M., N. Kanazawa, M. Selg, T. Samson, G. Roos, D. P. Reinhardt, R. Pabst, M. B. Lutz, and L. Sorokin. 2005. The conduit system transports soluble antigens from the afferent lymph to resident dendritic cells in the T cell area of the lymph node. *Immunity* 22: 19–29.
25. Eisenbarth, S. C. 2019. Dendritic cell subsets in T cell programming: location dictates function. *Nat. Rev. Immunol.* 19: 89–103.
26. Wendling, D. 2016. The gut in spondyloarthritis. *Joint Bone Spine* 83: 401–405.
27. Tiberio, L., A. Del Prete, T. Schioppa, F. Sozio, D. Bosisio, and S. Sozzani. 2018. Chemokine and chemotactic signals in dendritic cell migration. *Cell. Mol. Immunol.* 15: 346–352.
28. Joeris, T., K. Müller-Luda, W. W. Agace, and A. M. Mowat. 2017. Diversity and functions of intestinal mononuclear phagocytes. *Mucosal Immunol.* 10: 845–864.
29. Stagg, A. J. 2018. Intestinal dendritic cells in health and gut inflammation. *Front. Immunol.* 9: 2883.
30. Han, Y., X. Li, Q. Zhou, H. Jie, X. Lao, J. Han, J. He, X. Liu, D. Gu, Y. He, and E. Sun. 2015. FTY720 abrogates collagen-induced arthritis by hindering dendritic cell migration to local lymph nodes. *J. Immunol.* 195: 4126–4135.
31. Spiegel, S., and S. Milstien. 2011. The outs and the ins of sphingosine-1-phosphate in immunity. *Nat. Rev. Immunol.* 11: 403–415.
32. Maney, N. J., G. Reynolds, A. Krippner-Heidenreich, and C. M. U. Hilkens. 2014. Dendritic cell maturation and survival are differentially regulated by TNFR1 and TNFR2. *J. Immunol.* 193: 4914–4923.
33. Bieber, K., and S. E. Autenrieth. 2015. Insights how monocytes and dendritic cells contribute and regulate immune defense against microbial pathogens. *Immunobiology* 220: 215–226.
34. Itano, A. A., S. J. McSorley, R. L. Reinhardt, B. D. Ehst, E. Ingulli, A. Y. Rudensky, and M. K. Jenkins. 2003. Distinct dendritic cell populations sequentially present antigen to CD4 T cells and stimulate different aspects of cell-mediated immunity. *Immunity* 19: 47–57.
35. Neumann, B., A. Luz, K. Pfeffer, and B. Holzmann. 1996. Defective Peyer's patch organogenesis in mice lacking the 55-kD receptor for tumor necrosis factor. *J. Exp. Med.* 184: 259–264.
36. Bravo-Blas, A., L. Utriainen, S. L. Clay, V. Kästele, V. Cerovic, A. F. Cunningham, I. R. Henderson, D. M. Wall, and S. W. F. Milling. 2019. *Salmonella enterica* Serovar Typhimurium travels to mesenteric lymph nodes both with host cells and autonomously. *J. Immunol.* 202: 260–267.
37. Bottone, E. J. 1997. *Yersinia enterocolitica*: the charisma continues. *Clin. Microbiol. Rev.* 10: 257–276.
38. Watanabe, K., N. Watanabe, M. Jin, T. Matsuhashi, S. Koizumi, K. Onochi, M. Sawaguchi, S. Tawaraya, H. Miyazawa, H. Uchinami, et al. 2014. Mesenteric lymph node abscess due to *Yersinia enterocolitica*: case report and review of the literature. *Clin. J. Gastroenterol.* 7: 41–47.
39. Cargnelutti, E., J. L. Arias, S. R. Valdez, G. A. Rabinovich, and M. S. Di Genaro. 2013. TNFRp55 controls regulatory T cell responses in *Yersinia*-induced reactive arthritis. *Immunol. Cell Biol.* 91: 159–166.
40. Yang, S. K., Y. C. Wang, C. C. Chao, Y. J. Chuang, C. Y. Lan, and B. S. Chen. 2010. Dynamic cross-talk analysis among TNF-R, TLR-4 and IL-1R signalings in TNFalpha-induced inflammatory responses. *BMC Med. Genomics* 3: 19.
41. Hammer, G. E., E. E. Turer, K. E. Taylor, C. J. Fang, R. Advincula, S. Oshima, J. Barrera, E. J. Huang, B. Hou, B. A. Malynn, et al. 2011. Expression of A20 by dendritic cells preserves immune homeostasis and prevents colitis and spondyloarthritis. *Nat. Immunol.* 12: 1184–1193.
42. Anderson, A. O., J. T. Warren, and D. L. Gasser. 1981. Presence of lymphoid dendritic cells in thoracic duct lymph from Lewis rats. *Transplant. Proc.* 13: 1460–1468.
43. Jackson, D. G. 2019. Leucocyte trafficking via the lymphatic vasculature-mechanisms and consequences. *Front. Immunol.* 10: 471.
44. Schaper, K., M. Kietzmann, and W. Bäumer. 2014. Sphingosine-1-phosphate differently regulates the cytokine production of IL-12, IL-23 and IL-27 in activated murine bone marrow derived dendritic cells. *Mol. Immunol.* 59: 10–18.
45. Liu, K., G. D. Victora, T. A. Schwickert, P. Guermonprez, M. M. Meredith, K. Yao, F. F. Chu, G. J. Randolph, A. Y. Rudensky, and M. Nussenzweig. 2009. *In vivo* analysis of dendritic cell development and homeostasis. *Science* 324: 392–397.
46. Idzko, M., H. Hammad, M. van Nimwegen, M. Kool, T. Müller, T. Soullié, M. A. Willart, D. Hijdra, H. C. Hoogsteden, and B. N. Lambrecht. 2006. Local application of FTY720 to the lung abrogates experimental asthma by altering dendritic cell function. *J. Clin. Invest.* 116: 2935–2944.
47. Lan, Y. Y., D. Tokita, Z. Wang, H. C. Wang, J. Zhan, V. Brinkmann, and A. W. Thomson. 2008. Sphingosine 1-phosphate receptor agonism impairs skin dendritic cell migration and homing to secondary lymphoid tissue: association with prolonged allograft survival. *Transpl. Immunol.* 20: 88–94.
48. Lan, Y. Y., A. De Creus, B. L. Colvin, M. Abe, V. Brinkmann, P. T. Coates, and A. W. Thomson. 2005. The sphingosine-1-phosphate receptor agonist FTY720 modulates dendritic cell trafficking *in vivo*. *Am. J. Transplant.* 5: 2649–2659.
49. Zeng, X., T. Wang, C. Zhu, X. Xing, Y. Ye, X. Lai, B. Song, and Y. Zeng. 2012. Topographical and biological evidence revealed FTY720-mediated anergy-polarization of mouse bone marrow-derived dendritic cells *in vitro*. *PLoS One* 7: e34830.